



# Structural features and enhanced high-temperature oxygen ion transport in $\text{SrFe}_{1-x}\text{Ta}_x\text{O}_{3-\delta}$

Alexey A. Markov, Elizaveta V. Shalaeva, Alexander P. Tyutyunnik, Vasily V. Kuchin, Mikhail V. Patrakeev\*, Ilya A. Leonidov, Victor L. Kozhevnikov

Institute of Solid State Chemistry of Ural Branch of RAS, 91 Pervomaiskaya Str., 620990 Yekaterinburg, Russia

## ARTICLE INFO

### Article history:

Received 28 May 2012

Received in revised form

31 July 2012

Accepted 1 August 2012

Available online 15 August 2012

### Keywords:

Ta-substituted strontium ferrite

Local inhomogeneities

Double perovskite

Phase separation

Oxygen non-stoichiometry

Ion conductivity

## ABSTRACT

Structural features, oxygen non-stoichiometry and transport properties are studied in the oxide series  $\text{SrFe}_{1-x}\text{Ta}_x\text{O}_{3-\delta}$ , where  $x=0.2, 0.3$  and  $0.4$ . X-ray diffraction and electron microscopy data evidence formation of the inhomogeneous materials at  $x=0.3$  and  $0.4$ , which include phase constituents with a cubic perovskite and a double perovskite structure types. The composition, the amount and the typical grain size of the phase inhomogeneities are shown to depend both on doping and oxygen content. The increased oxygen-ion conductivity is observed in oxygen depleted materials, which is explained by the increase in the amount of cubic perovskite-like phase and development of interfacial pathways favorable for enhanced oxygen ion transport.

© 2012 Elsevier Inc. All rights reserved.

## 1. Introduction

Mixed, oxygen ion and electron, conducting oxides have a potential of important applications such as materials for solid oxide fuel cells, sensors, oxygen separation and natural gas processing [1–4]. The strontium perovskite-like ferrite  $\text{SrFeO}_{3-\delta}$  is notorious among them for high level of oxygen semi-permeability, which is provided by appreciable contributions to conductivity from both ions and electrons [5,6]. Also, this ferrite exhibits rather satisfactory stability toward reduction [7]. The most serious material drawback that deleteriously affects transport characteristics is the tendency of oxygen vacancies in the ferrite to ordering [8]. Moreover, the vacancy ordering eventually results in the phase transition from a perovskite to a brownmillerite type structure, and dimensional changes that accompany this transition favor fracturing and loss of integrity of ferrite coatings and ceramics [9].

It is known that partial replacement of iron in  $\text{SrFeO}_{3-\delta}$  for other cations often leads to suppression and complete disappearance of the phase transition [10–12]. However, other doping effects may differ significantly depending on the dopant nature. Thus, scandium introduction into the crystalline lattice is useful to maintain the cubic structure while oxygen ion and electron transport parameters decrease rapidly with the increase of

scandium content [13]. The substitution of iron for aluminum is similarly beneficial for stabilization of the cubic structure. However, in difference with the scandium doping replacement of iron for aluminum may result in even better transport characteristics in the doped derivatives than in the parent ferrite [14]. It is suggested [15] that the maintenance of the cubic structure at doping is closely related with peculiar structural changes on a small scale so that the perovskite-like ferrite matrix occurs interspersed with defect associates. The structural architecture of the defect clusters and their developed interface with the surrounding perovskite matrix may significantly influence ion transport owing to strong interfacial disordering [16]. Whether the interface is rigid or change with external conditions is not quite clear.

$\text{Ta}^{5+}$  and  $\text{Fe}^{3+}$  cations are of about the same size and readily adopt octahedral oxygen coordination in solid state oxides, which is favorable for formation of extended solid oxide solutions. When half of iron in  $\text{SrFeO}_{3-\delta}$  is replaced for tantalum the stoichiometric double perovskite type oxide  $\text{Sr}_2\text{FeTaO}_6$  is obtained where iron maintains 3+ oxidation degree [17]. At the same time, the substituted ferrite with  $\text{Ta/Fe} < 1$  is expected to contain oxygen vacancies and iron in a mixed oxidation state; both features favor mixed conductivity. It is important also that tantalum–oxygen chemical bonding is one of the strongest as can be seen from oxygen vacancy formation enthalpies in oxides [18]. Therefore, doping is expected to enhance the ability of  $\text{SrFeO}_{3-\delta}$  to withstand harsh environments. Indeed, it is shown [19,20] that tantalum substitution in  $\text{La}_{0.5}\text{Sr}_{0.5}\text{FeO}_{3-\delta}$  results in decreased isothermal expansion and increased stability in reducing conditions. Accordingly, the aim of this work was to study the

\* Corresponding author. Fax: +7 343 3744495.

E-mail address: [patrakeev@ihim.uran.ru](mailto:patrakeev@ihim.uran.ru) (M.V. Patrakeev).

influence of tantalum doping on crystalline structure features, oxygen non-stoichiometry and high-temperature transport in moderately doped  $\text{SrFe}_{1-x}\text{Ta}_x\text{O}_{3-\delta}$ .

## 2. Experimental

The high-purity grade oxides  $\text{Fe}_2\text{O}_3$ ,  $\text{Ta}_2\text{O}_5$  and strontium carbonate  $\text{SrCO}_3$  were used as reagents for solid state synthesis of  $\text{SrFe}_{1-x}\text{Ta}_x\text{O}_{3-\delta}$ , where  $x=0.2, 0.3$  and  $0.4$ . The reagents were calcined at appropriate temperatures prior to their using in order to remove adsorbates. The desirable amounts of the starting materials were carefully mixed with a mortar and pestle. The mixtures were pressed into pellets under uniaxial pressure of 1 kbar, fired in air at  $1000^\circ\text{C}$  during 10 hours and cooled with the rate of  $5^\circ/\text{min}$  to room temperature. The procedure of heat treatment was repeated several times with intermittent grindings, pelletizations, and gradual increase of the synthesis temperature to  $1350^\circ\text{C}$ . The apparent density of the obtained specimens was about 93% of theoretical.

X-ray powder diffraction was used for the phase purity control and determination of the crystal lattice parameters in the obtained samples with the help of a STADI-P (STOE) diffractometer ( $\text{CuK}\alpha$ -radiation). The scan range was  $2\Theta=15\text{--}120^\circ$  with  $\Delta\Theta$  step  $0.03^\circ$  and counting for 60 s at each step. Polycrystalline silicon was used as an external standard ( $a=5.43075(5)\text{\AA}$ ). The lattice parameters and volume fraction of phases were determined from the XRD data with the help of a PCW 2.4 calculation package.

The oxygen content variations in the doped ferrites were measured in the isothermal mode at  $950^\circ\text{C}$  with the using of a coulometric titration technique within the limits  $10^{-16}\text{--}0.5$  atm of oxygen partial pressure [21]. Additional measurements for the sample  $x=0.4$  were carried out at several temperatures within  $800\text{--}950^\circ\text{C}$ . The specimens with oxygen content  $3-\delta=2.5+x$  (hereafter, reduced samples for contrasting with air-prepared, oxidized samples) were obtained by equilibration of the as-synthesized samples in the sealed coulometric titration cell at  $950^\circ\text{C}$  and  $p_{\text{O}_2}\sim 10^{-10}$  atm followed by cooling to room temperature. The obtained reduced powder specimens were treated in the isobutyl alcohol bath with ultrasonic stirring, and then used to form sediments upon a carbon film. The film with deposited sediments was supported with a copper grid for electron microscopy studies (JEM-200 CX and CM-30 Philips). Simulated electron diffraction patterns were obtained with the help of a CarIne Crystallography 40 software.

The rectangular bars  $12\times 2\times 2$  mm cut from the sintered pellets were used for 4-probe d.c. conductivity measurements as described elsewhere [22]. The measurements were carried out in isothermal conditions with stepwise changes of oxygen partial pressure. The oxygen pressure interval  $10^{-10}\text{--}10^{-5}$  atm is characterized by exceedingly slow kinetics of equilibration of specimens with the surrounding  $\text{CO}/\text{CO}_2$  gas mixture in the measuring cell and, consequently, by poor reliability of the data at moderate temperatures [23]. Therefore, this pressure range was skipped during measurements below  $950^\circ\text{C}$ , and the entire span of pressure variations was covered only during measurements at  $950^\circ\text{C}$  where the equilibration kinetics is quite fast at any pressure.

## 3. Results and discussion

### 3.1. Structural features

The X-ray powder diffraction patterns show main reflections characteristic for a cubic perovskite-like structure (s.g.  $Pm\bar{3}m$ ) in the air synthesized samples  $\text{SrFe}_{1-x}\text{Ta}_x\text{O}_{3-\delta}$ , where  $x=0.2$  and  $0.3$ . The reducing treatment at  $p_{\text{O}_2}\sim 10^{-10}$  atm and  $950^\circ\text{C}$  does

not change the apparent cubic symmetry of the doped samples in striking difference with the parent ferrite, which acquires the orthorhombic brownmillerite structure (s.g.  $Ibm2$ ) [24]. The cubic elementary unit parameter increases with tantalum content, Fig. 1. The increase in the doping to  $x=0.4$  results in the lattice parameter somewhat smaller than expected from the Vegard's law. Careful examination of the diffraction pattern reveals very weak super-structure reflections, Fig. 2(a). The reflections are characteristic for the double perovskite phase  $\text{Sr}_2\text{Fe}_{2(1-y)}\text{Ta}_2\text{O}_6$  where the perovskite-like lattice parameter is smaller compared

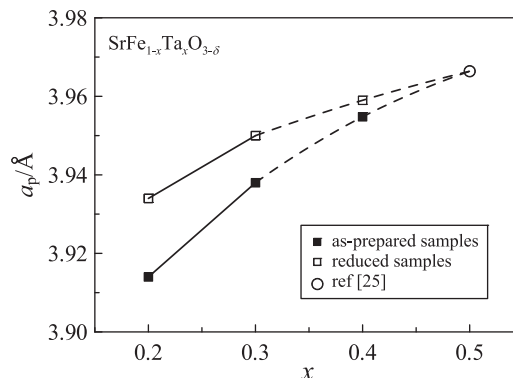


Fig. 1. The changes with tantalum content of crystalline lattice parameters in air prepared and reduced samples  $\text{SrFe}_{1-x}\text{Ta}_x\text{O}_{3-\delta}$ .

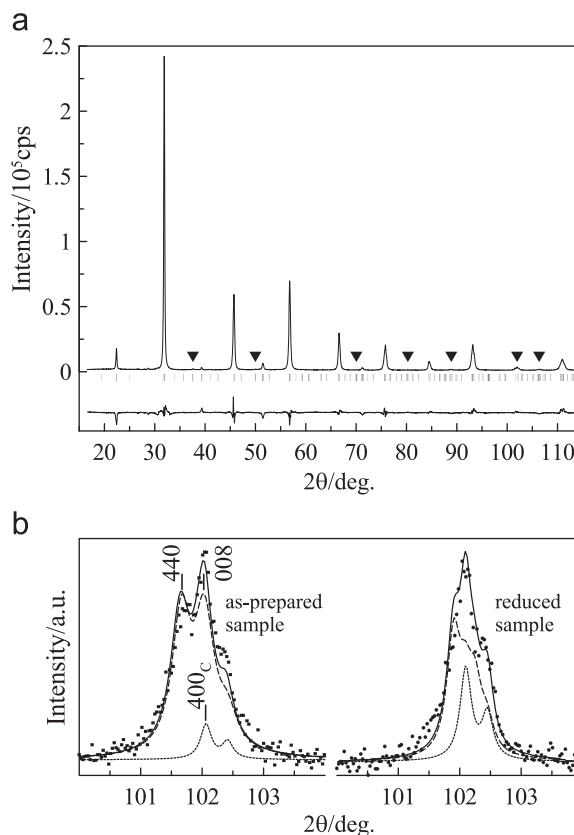


Fig. 2. The experimental X-ray powder diffraction pattern and the profiles calculated with a two-phase model for  $\text{SrFe}_{0.6}\text{Ta}_{0.4}\text{O}_{3-\delta}$ . (a)— $2\Theta$  range is  $15^\circ\text{--}120^\circ$ , dots and solid line show experimental and calculated results, respectively. Symbols ▼ mark superstructure reflections. (b)—deconvolution of the diffraction reflections at  $2\Theta=100^\circ\text{--}104^\circ$  for air-prepared and reduced samples. The dot line shows the profile for the cubic perovskite  $(400)_{\text{cub}}$  reflection. The dashed line shows the profile for reflections  $(440)_{\text{dp}}$  and  $(008)_{\text{dp}}$  of the double perovskite phase.  $R_p=5.91$ ,  $R_{\text{wp}}=8.7$ ,  $R_{\text{exp}}=1.74$ .

Download English Version:

<https://daneshyari.com/en/article/1330095>

Download Persian Version:

<https://daneshyari.com/article/1330095>

[Daneshyari.com](https://daneshyari.com)